AIMS Geosciences

AIMS Geosciences, 10(4): 864–881.
DOI: 10.3934/geosci.2024040
Received: 11 July 2024
Revised: 30 August 2024
Accepted: 29 September 2024
Published: 01 November 2024

https://www.aimspress.com/journal/geosciences

Review

A «necklace» of large clusters of strategic raw materials over a stagnant oceanic slab in East Asia

Natalia Boriskina*

Far East Geological Institute, Far Eastern Branch of Russian Academy of Sciences, 159 pr-t 100 let Vladivostoku, Vladivostok, Russia

*** Correspondence:** Email: boriskina2000@mail.ru; Tel: +7-924-237-3038.

Abstract: An analysis of geological-geophysical, metallogenic, geochronological, and seismic tomographic studies in territories joining Southeast Russia, East Mongolia, and Northeast China led to the conclusion that deep geodynamics significantly influenced the formation of highly productive ore-magmatic systems in the Late Jurassic-Early Cretaceous. This influence was likely manifested through the initiation of decompression processes around stagnant slab boundaries in the Late Mesozoic. Decompression and advection, which are particularly active near the natural boundaries of the slab, act as triggers for the intense interaction of under and over subduction asthenospheric fluids with adjacent sections of the mantle and for the directed upwelling of powerful flows of matter and energy into the lithosphere. These flows determine the locations of intermediate and peripheral magma chambers: Primary chambers in the lower lithosphere among the metasomatized mantle and lower crust and associated chambers in the middle and upper cratonized parts of the lithosphere. Large ore clusters containing noble metals (Au, PGE), uranium, fluorite, and Cu-Mo-porphyry deposits are associated with late- and postmagmatic derivatives of the emerging magma chambers over the frontal and peripheral (paleotransform) boundaries of a stagnant Pacific slab. These large Late Mesozoic ore clusters and districts form a distinctive “necklace” of strategic materials in East Asia.

Keywords: slab subduction; East Asia; Late Mesozoic ore clusters; noble metal; uranium; fluorite; and Cu-Mo-porphyry deposits

1. Introduction

The territories joining Southeast Russia, East Mongolia, and Northeast China, collectively referred to as Priamury, occupy a significant part of East Asia. Geologically, this area is a zone where the fold structures of the Central Asian (Ural-Mongol) and Pacific Orogenic Belts converge, bounded to the north and south by the Siberian (North Asian) and Sino-Korean (North China) cratons, respectively (Figure 1).

In Priamury, areas where deposits of noble, nonferrous, and radioactive metals of Late Mesozoic age are concentrated display not only clustered (nodal) but also linear (belt-like) arrangements [1–3]. Ore-forming processes in many mineragenically specialized clusters and districts, which spread hundreds and thousands of kilometers apart, are characterized by similar evolutionary trends and relative synchronicity in formation, despite being part of different tectonic structures. [4–7]. These ore-forming processes are associated with high alkalinity magmatic formations of the Late Jurassic-Early Cretaceous age. Identifying the characteristics of the geodynamic environments in which these deposits formed is important both scientifically and practically. Furthermore, the number of the largest world-class ore clusters and districts in the worldwide is relatively small.

My purpose of this review is to provide evidence of the influence of deep geodynamics on the significant development of ore-forming processes in certain environments and to identify the prerequisites for subsequently applying this concept in metallogenic zonation, as well as in exploratory research.

An analysis and synthesis of geological and geophysical data on regional metallogeny in Priamury, in conjunction with geochronological and tomographic research materials on the Late Mesozoic-Cenozoic deep geodynamics in East Asia, will enable a reevaluation of the major factors that influenced the formation and location of large and super large ore clusters with Au, PGE, U, Mo, and fluorite mineralization.

2. Geological and geophysical characteristics of the study area

The Priamury region, located within the Asian continent and situated between the Siberian and Sino-Korean cratons, is also distinguished as the Amur plate [8]. This plate is a collage of microcontinents featuring Early Precambrian sialic crust separated by orogenic (fold-thrust) superterranes of various ages made up of transformed rock complexes from passive and active margins, marked by ophiolitic sutures [7,9–11]. The largest super terranes in the region, which belong to the Central Asian Orogenic Belt, include Baikal-Vitim, Selenga-Stanovoi, Mongol-Okhotsk, Solonker, and South-Mongol (Figure 1). Fragments of fold-thrust structures in the Pacific belt are represented by the Badzhal and Sikhote-Alin super terranes. Among the Priamury super terranes, the most notable are Kerulen-Argun, South Gobi, and Bureya-Jiamusi-Khanka. A distinctive feature of the region is a large Late Mesozoic igneous province, which includes layered systems of volcanic-plutonic belts (VPB) and volcanic-plutonic zones (VPZ), extensive rift depressions, syneclises, and broad fields of Cenozoic plateau basalts. Notably among the VPB are Mongolia-Priargun, Greater- and Lesser Xingan, and East-Sikhote-Alin; among the VPZ are Badzhal, Umlekan-Ogodzha, Lower Zeya, and Ichun-Yuquan. The marginal continental VPBs and their

segments include East-Sikhote-Alin, Uda-Murgal, and Okhotsk-Chukotsk. Among the rifts and grabens, the largest are Songliao, Amur-Zeya, Sangjian-Middle-Amur, Syaolihe, Hulunur, Erlian, and Dzunbain.

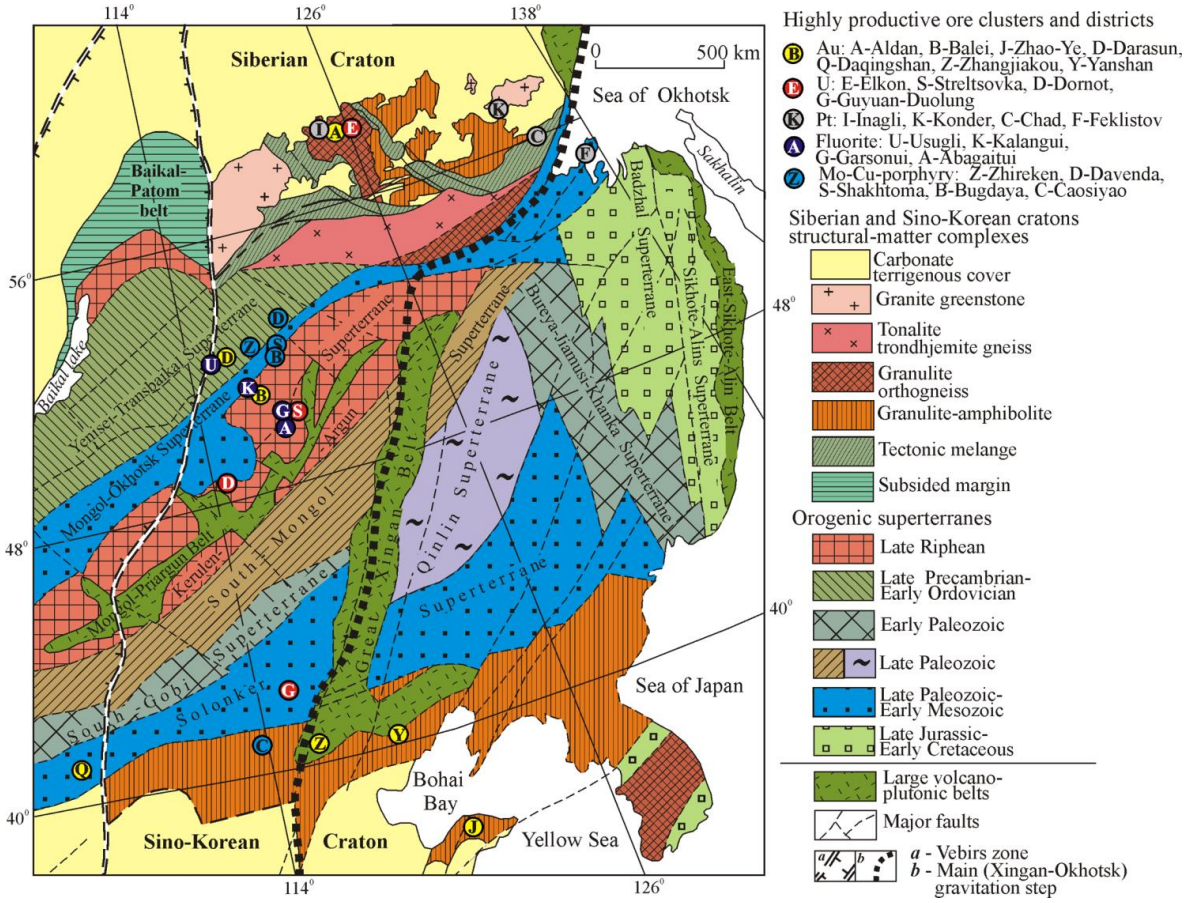

Figure 1. Highly productive ore clusters and districts of East Asia on a tectonic framework. Modified with additions after [4,9,10].

The Priamury region exhibits abnormally high heterogeneity in its crust and mantle. It prominently features rifting accompanied by the basification of the Earth's crust along the axial zones of depressions and the formation of Cenozoic areas of basaltic volcanism. The region is also characterized by increased elevated seismic activity [10,12–14]. A significant regional geological feature is the Xingan-Okhotsk fragment of the Indo-China-Chukotka (Main) gravity domain, which is approximately 150 km wide with a gravitational difference of 50–100 mGal and a total length of over 3000 km [10,13]. To the east of the Xingan-Okhotsk fragment of the Main gravity domain, the crust of Priamury is thinner, measuring 32–34 km, whereas to the west, the crust thickness increases by 10–12 km. In the western area, the lithosphere thickness also increases to approximately 150 km, whereas in the east, it decreases to 80 km [10].

Another significant geological division in the region is the Vebirs zone (Verkhoyan-Birma), which is of Late Paleozoic-Early Mesozoic origin. This zone represents the virtual western boundary of East Asia, where the influence of the Pacific Mobile Belt structures ends. In Southeast Russia, the Vebirs zone is represented by the Baikal fragment, which is 400–500 km wide and includes several extended near-meridional faults and parts of Phanerozoic fold systems enclosed between them. The Baikal and Khubsugul rifts are confined to the axial part of the zone, as is the so-called prerift area [15],

in which diatremes, dikes, and subvolcanic bodies composed of alkaline basalt rocks are known to exist in Mongolia, south of the Tunkin Valley. A consistent weakening of the influence of Mesozoic-Cenozoic geodynamics from east to west is recorded in the Vebirs zone. The eastern border of the zone coincides with the Patom-Zhuya and Onon-Tura deep strike-slip faults in Transbaikalia and with the East-Gobi and Dzunbain depressions in Mongolia. Near this zone, belts of Late Jurassic-Early Cretaceous magmatism are prominent: the Aldan belt of alkaline intrusions; the Nercha-Oldoi, Mongol-Priargun, and South-Gobi basalt-rhyolite belts; and systems of rift basins synchronous with them [10]. Manifestations of Mesozoic granitoid magmatism and contrasting basalt-rhyolite associations, as well as Lower Cretaceous coal-bearing depressions, completely disappear at the western boundary of the Vebirs zone.

3. Paleotectonic reconstructions and seismic tomography data

The concept of the geodynamic evolution of a region is based on the integral model of the active continental margin [9,16,17]. Many scientists agree that the major events in the formation of the structure of East Asia occurred in the Jurassic-Cretaceous and Cenozoic [18–20]. The eastern flank of the Central Asian Orogenic Belt in the Asia Pacific convergence zone was “opposed” by the most ancient part of the paleo-Pacific plate [21]. The active development of subduction and rifting processes in the zone led to the emergence of several fragments of the Asian continental margin-related volcano-plutonic belt [22.23]. On the basis of geophysical data of the Main gravity domain location, such fragments in the Late Jurassic-Early Cretaceous evolution of the region were Uda-Murgal, Umlekan-Ogodzha, and Great Xing’an VPB. There are several alternative viewpoints regarding the Great Xing’an belt. Some geologists consider it intracontinental [9,20], while others interpret it as a continental margin-related belt [11,24,25], with some differences in the interpretation of the spatial position of the paleo-subduction zone associated with the formation of the Great Xing’an VPB. The author concurs with Gordienko [26], who reported that the subduction zone near the VPB is likely buried under the Songliao syneclise of rifting origin. To a certain extent, this is confirmed by the presence of local mantle and asthenosphere uplifts, seismic activity, and elevated heat flow. The thinned lithosphere of the syneclise resembles that of the riftogenic trough along the coasts of the Okhotsk and Japanese margin seas [10]. With such an interpretation, the Late Mesozoic volcanic zones of Eastern Transbaikalia, and perhaps the entire Mongol-Priargun belt, are external peripheral fragments of the large Upper Amur VPB, of which the Great Xing’an belt was its internal (axial) part. This interpretation of geological and geophysical materials completely agrees with the results of many geochronological [27–29], petrological, geochemical [30,31], and metallogenic studies [20,32,33] and relatively simply explains the reason for the convergence of the Argun-Gonzha and Selenga-Stanovoi composite terranes in the Early Jurassic, followed by the subsequent “die-off” (closure) of the Transbaikal and Upper Amur segments of the Mongol-Okhotsk oceanic basin. It is also possible that the convergence ended at the beginning of the Middle Jurassic during the collision of the Aldan-Stanovoi and Amur plates [34]. Judging from numerous isotopic age determinations of magmatites distributed in different parts of the Upper Amur VPB, its active development terminated by the end of the Early Cretaceous or somewhat later [35,36].

In the Late Cretaceous (100–75 Ma) along the eastern margin of Asia (from Southern China to the Siberian Craton), a western fragment of the Pacific plate, represented by the Izanagi Plate,

predominantly underwent frontal subduction. This subduction process contributed to the formation of the East Sikhote-Alin arc and other magmatic arcs of the VPB, as well as the development of forearc (West Sakhalin and others) and backarc (Sanjiang-Middle Amur, Alchan, Lower Amur, etc.) rift troughs filled with volcanic-sedimentary molasse complexes. The Pribrezhnaya gradient zone, associated with East Sikhote-Alin VPB, has approximately the same variance in gravity field anomalies as Xingan-Okhotsk.

Subsequently, in the Maastrichtian-Eocene, following the absorption of the Izanagi Plate, another intensification of transform (or strike-slip) activity between the Eurasian and Pacific plates occurred. This led, in the Oligocene-Miocene, to new counter-movements and the emergence of the Kuril and Japanese island arcs. Intense rifting during this period, which resulted in the stretching and thinning of the crust, led to the formation of the Sea of Okhotsk and the Sea of Japan, as well as extensive fields of high-alkalinity plateau basalts (Figure 2).

The information provided about the existence of Late Mesozoic-Cenozoic magmatic formations of crust-mantle origin in Southeast Russia, East Mongolia, and Northeast China highlights the need for modern analysis of tomographic study results. On the basis of these data [12,32,37–42] and paleotectonic reconstructions, the subduction processes of the Pacific plate beneath the Eurasian continent have been actively developing since the Late Mesozoic. As the Pacific megaplate fragments subsided into the mantle, they transformed within the transition zone into a stagnant heterochronic composite slab (Figure 3). The slab front, which aligns well with the western contour of the large post-riftogenic Mesozoic-Cenozoic depression distribution and extensive fields of Cenozoic basalts, is projected onto the Aldan and Olekma interfluves, including their middle and upper reaches, and extends further to Southeastern Transbaikalia, East Mongolia, and Northeast China. Considering studies of the Sakhalin-South Kuril Province [43], there is reason to believe that the WNW-oriented slab flank boundaries may have been paleotransform faults preserved beneath the continent and active during subduction processes. Notably, on the present-day surface, the width of the areas where mantle formations are mapped, i.e., in the belt of probable influence of both the frontal and flank boundaries of the slab, reaches 150–200 km. [6,44]. This finding is consistent with the transverse dimensions of similar faults established by researchers examining thermal fields in the Atlantic and southeast Pacific [45].

4. Generalized description of large clusters of strategic raw materials in East Asia

East Asia covers an area of approximately 1 million square kilometers and is situated between the Siberian and North China platforms. It is bounded to the west by the Baikal fragment of the Vebirs zone and to the east by the coasts of the Sea of Okhotsk and the Sea of Japan. Currently, more than a dozen superlarge, world-class ore clusters of the Late Jurassic-Early Cretaceous age are known in this region. These deposits include gold deposits—Aldan, Balei (Russia), and Zhao-Ye (China); uranium deposits—Elkon, Strelzovka (Russia), and Dornot (Mongolia); placer deposits, mainly platinum metal deposits—Inagli, Konder, Feklistov, and Chad (Russia). Additionally, large Mo-porphyry deposits (Bugdaya, Shakhtama, Davenda, Zhireken, Caosiyao), Cu-Mo deposits (Kultuma), and fluorite veins (Garsonui, Kalangui, Usugli, Abagaitui, etc.) have been discovered within the same territory. Information about their ages is provided in Table 1.

Strategic raw material reserves in the listed deposits, depending on their association with specific

ore-magmatic systems (OMS) and metallogenic specialization, exceed dozens to hundreds of tons of PGE, thousands of tons of Au, dozens to hundreds of thousands of tons of uranium, hundreds of thousands to millions of tons of Mo, and millions to tens of millions of tons of fluorite [4,20,46,47].

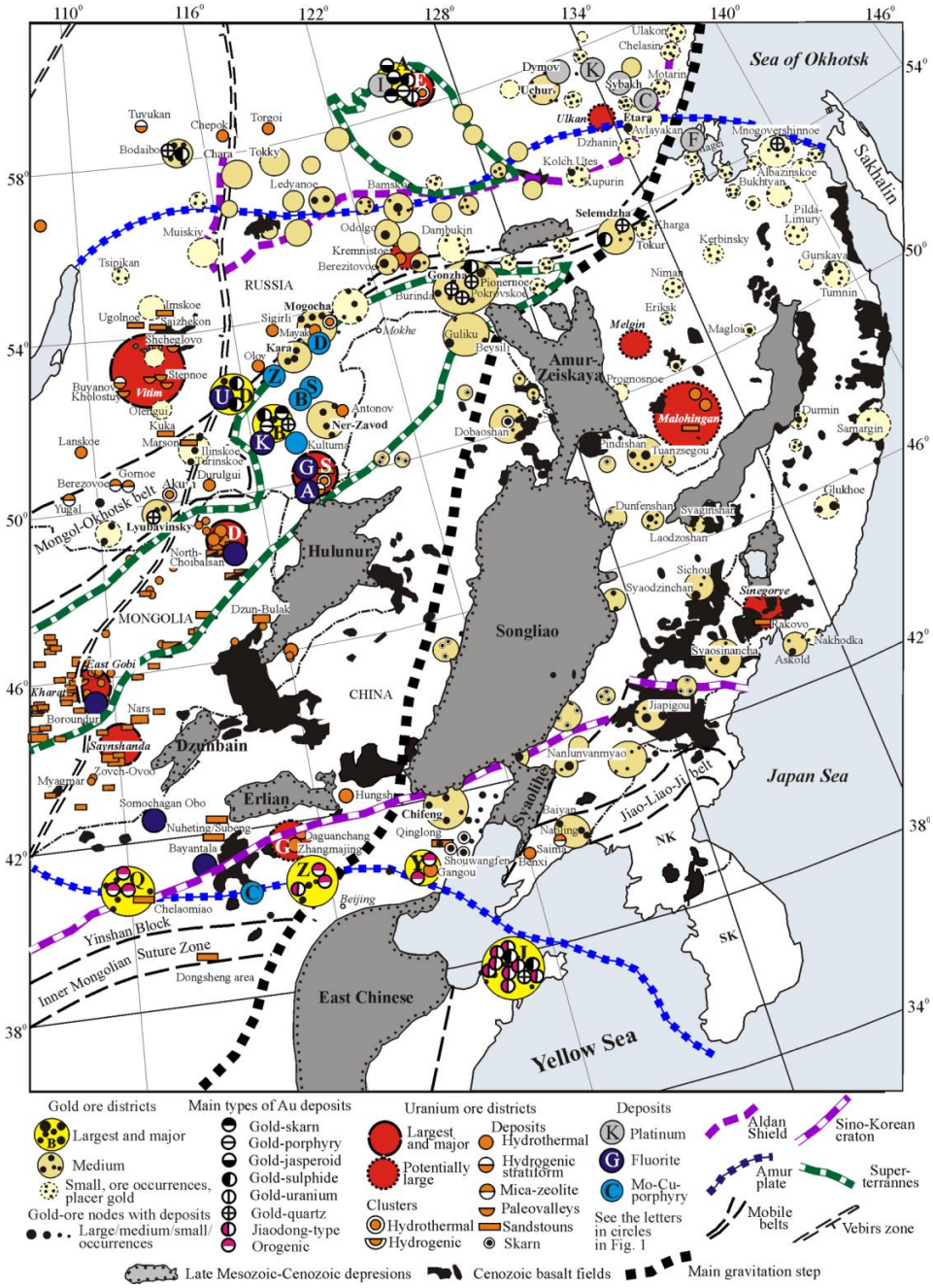

Figure 2. The location of strategic raw materials in relation to the Late Mesozoic and Cenozoic rift-related depressions and large fields of highly alkaline plateau basalts. After [1,4,6,8,10,12,44,48] with modifications and additions.

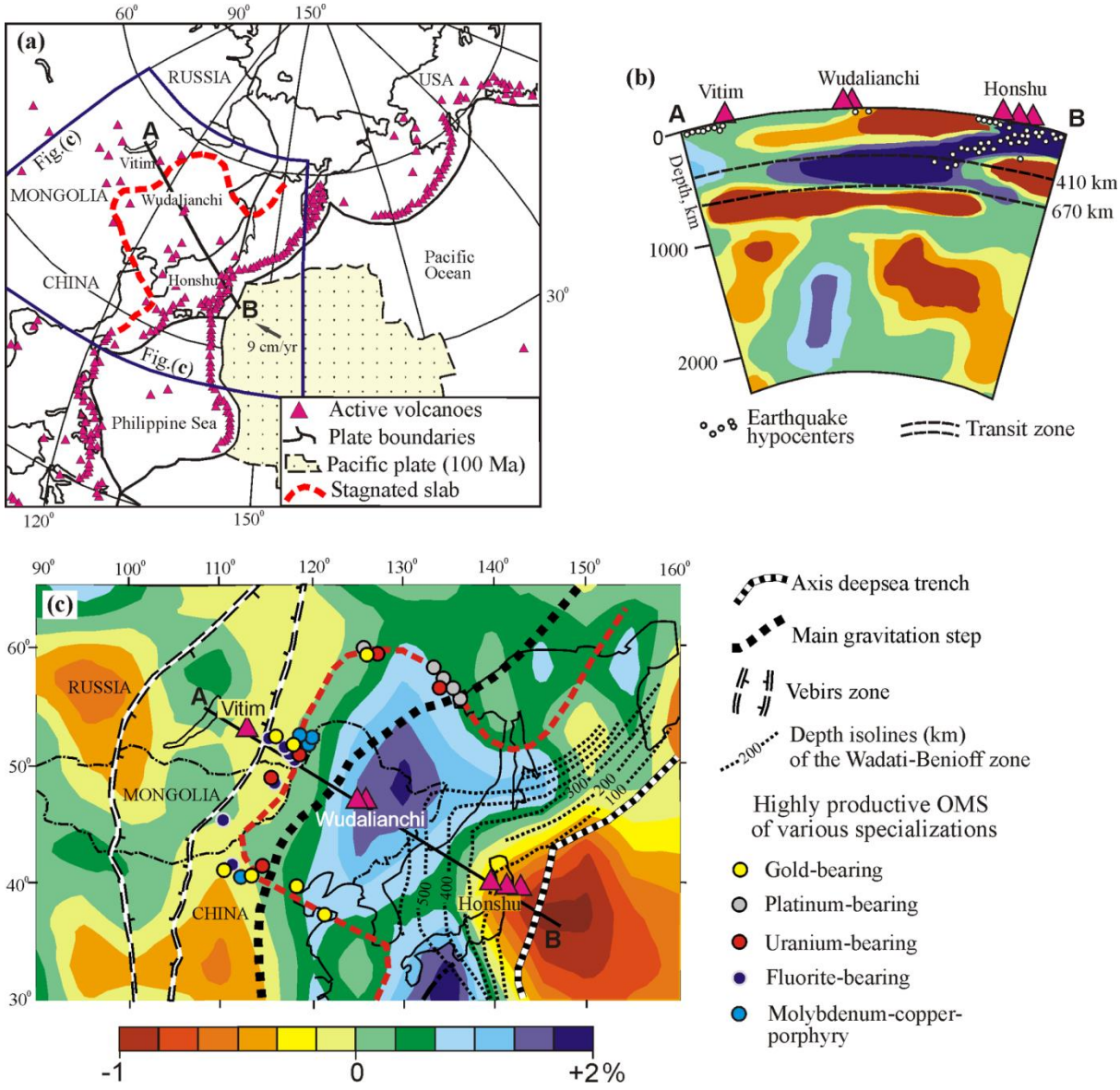

Figure 3. (a) Part of the Asia-Pacific convergence megazone. (b) Section of mantle along profile along line AB showing the stagnant slab in the mantle transit zone. (c) Distribution of seismic anomalies (100ΔVp/Vp%) at a depth of 550 km and velocity scale for longitudinal seismic waves. After [4–6,32,49] with modifications.

The common features of the listed ore clusters and districts include their locations on the edges of cratons or cratonized terranes with crustal thicknesses of 36–38 km near large gravity gradients and tectonic mélange zones [50]. These objects are characterized by their association with Late Mesozoic (Middle-Late Jurassic-Early Cretaceous) mafic and/or salic magmatic, high alkalinity formations—derivatives of deep (crust-mantle) layered chambers (magmatogens), which act as important indicators of highly productive OMS. The affiliation of large clusters and districts with such OMS is determined by the sequential localization of magma and ore-forming process derivatives in their area and their zoned position. This includes, on the one hand, intrusive and subvolcanic bodies, dikes, and on the other hand, depending on specialization—Mo-porphyry or

Mo-U, Li, fluorite, Au-rare metal (with Te, Bi, W), Au-U-quartz, Au-sulfide, Au-porphyry, Au-Ag, and Au-jasperoid deposits. Zonation is combined with an increase in the content of noble metals (up to extremely high levels) in later ore bodies: stockworks and linear vein bodies [4,30]. In each district of concentration, both noble metals and uranium, as well as molybdenum mineralization, show evidence that Late Jurassic-Early Cretaceous mineralization was inherited from earlier stages, as identified among the Archean greenstone, Riphean metamorphic, and Paleozoic granitoid formations [5,51–53]. The listed ore clusters and districts include deposits from three evolutionary series: Gold-molybdenum, rare-polymetal-uranium, and fluorine-gold-silver.

Table 1. Formation time of highly productive OMS of various specializations over a stagnant slab in East Asia.

Metallogenic specialization of OMS	Typical ore clasters and districts	Age (Ma)	Dating method	References
Gold-bearing	Aldan (South Yakutia, Russia)	165 – 155, 145 – 140, 135 – 130	K-Ar (magmatites)	[54,55]
	Darasun (South Transbaikalia, Russia)	160.5 ± 0.4	Rb-Sr (granodiorite porphyry)	[56]
		159.6 ± 1.5	K-Ar (beresites)	
	Balei (Transbaikalia, Russia)	175 ± 6, 148 ± 6, 120 ± 5	K-Ar (metasomatites)	[31,57,58]
	Daqingshan (North China Craton (NCC))	239.8 ± 3.0	Ar-Ar (sericite)	[33]
	Zhangjiakou (NCC)	389 ± 1; 135.5 ± 0.4	U-Pb (zircon)	
	Yanshan (NCC)	199 ± 2;	U-Pb (zircon)	
		192 – 177	Re-Os (molybdenite)	
	Zhao-Ye (Jiaodong Peninsula, China)	121.0 ± 2.0	Ar-Ar (sericite)	
		120.6 ± 0.9	Rb-Sr (pyrite)	
		159 ± 1; 116 – 132; 149 ± 5, 129 ± 1; 117 ± 3	U-Pb (zircon)	
Platinum-bearing	Inagli (South Yakutia, Russia)	145.8 ± 3.2; 142.4 ± 2.0; 133.4 ± 1; 133 – 128;	Ar-Ar (clinopyroxenite)	[59,60]
	Chad (Khabarovsk district, Russia)	123 ± 6; 113 ± 6; 107 ± 6	^{90}Pt–^{4}He (isoferroplatinum)	[61–63]
	Konder (Khabarovsk district, Russia)	124.9 ± 1.9	U-Pb (baddeleytte)	
		125.8 ± 3.8	U-Pb (zircon)	
		112 ± 7	^{90}Pt-^{4}He (isoferroplatinum)	
		129 ± 6	^{90}Pt-^{4}He (isoferroplatinum)	[64]

Continued on next page

Metallogenic specialization of OMS	Typical ore clasters and districts	Age (Ma)	Dating method	References
Uranium-bearing	Elkon (South Yakutia, Russia)	150 – 130	K-Ar(magmatites)	[65,66]
		135 – 130	Rb-Sr (granodiorite porphyry)	
	Streltsovka (South Transbaikalia, Russia)	178 – 154;150 – 138; 126 – 117	U-Pb (zircon), Rb-Sr (rhyolites, granites)	[31,51]
		144 ± 5; 138 ± 5; 129 ± 5	K-Ar (hydromicasite)	[57]
	Dornot (East Mongolia)	172 – 168; 161 ± 7	K-Ar (hydromicasite)	[31,51,67]
		170 – 160; 145 – 143;		
		139 ± 2	Rb-Sr (granites)	
		138 – 135	U-Pb (zircon)	
	Guyuan-Duolung (Inshan-Liaohe, China)	132.6 ± 8,9~136.4 ± 3,1	Rb-Sr (rhyolite)	[68]
		136.2 ± 2.9;	U-Pb (zircon)	[69,70]
		140.2 ± 1.6; 138.6 ± 1.4		
Fluorite-bearing	Usugli (South Transbaikalia, Russia)	120 – 110 ± 5	K-Ar (muscovite)	[71]
	Kalangui (South Transbaikalia, Russia)	114 – 112		
	Garsonui (South Transbaikalia, Russia)	165 ± 9	K-Ar (muscovite)	[31,57]
	Abagaitui (South Transbaikalia, Russia)	135 ± 6		
Molybdenum-copper-porphyry	Zhireken (Eastern Transbaikalia, Russia)	161.0 ± 1.6; 157.5 ± 2.0	U-Pb (zircon)	[52,72,73]
		163 ± 1	Re-Os (molybdenite)	
	Shakhtama (Eastern Transbaikalia, Russia)	160 – 157	Re-Os (molybdenite)	
		163 – 159, 160 – 153	U-Pb (zircon)	
	Bugdaya (Eastern Transbaikalia, Russia)	136 ± 7	K-Ar (beresites)	[57]
	Caosiyao, (Xinghe, Inner Mongolia, China)	128.6 ± 2.4; 150.9 ± 2.2	Re-Os (molybdenite)	[29]
		140.1 ± 1.7; 148.5 ± 0.9	U-Pb (zircon)	

5. Discussion

The Aldan ore district is key to understanding the general patterns of strategic raw material deposit distributions in East Asia. It features several gold-bearing zones [54], and a significant number of uranium-bearing zones [53], alongside concentrations of molybdenum occurrences and deposits, as well as the presence of fluorite in the Elkon ore district. Notably, the platinum-bearing alluvial deposits along the Inagli River and its tributaries are also recognized [1]. The source of the

platinum group minerals in the Inagli River placers is the zoned alkaline ultramafic Inagli pluton, the dunite core of which is encased by Late Mesozoic varieties high in silica and alkalis. Additionally, other zoned platinum-bearing alkaline ultramafic massifs similar to Inagli (e.g., Konder, Feklistov, Chad, etc.), featuring placers of Au and platinum group minerals, were identified to the ESE of the Aldan district in the Inagli-Konder-Feklistov magma-metallogenic belt, which stretches over 1000 kilometers (Figure 4) [1,5].

There is petrological and isotope-geochemical evidence supporting the mantle origin of mafic-ultramafic complexes in the listed zoned massifs, as well as the Cr-PGE mineralization identified here [59,74,75]. The age of its formation, dated for native Pt minerals from the Konder massif (^{190}Pt-^{4}He method) is 112 ± 7 Ma [61]; the ^{190}Pt-^{4}He ages of isoferroplatinum samples of different geneses –129 ± 6 Ma [63]; and the ages of baddeleytte and zircon (U-Pb method) from the dunite core are 124,9 ± 1,9 and 125,8 ± 3,8 Ma, respectively [62]. The data presented are quite comparable to the concentrations of gold, uranium, uranium-molybdenum, molybdenum, copper-molybdenum, and fluorite mineralization in East Asia (see Table). Generally, fluorite not only is a typomorphic mineral in U, Mo-U, and Cu-Mo deposits [76] but also forms significant fluorite deposits in many ore clusters in Transbaikalia and Mongolia.

When the seismic tomographic and minerogenic layouts of Priamury are combined, the largest ore clusters, districts, and fields of Au, PGE, U, as well as Mo and fluorite, are in the region over the front and flank boundaries of the stagnant oceanic slab (Figure 4). The emergence of highly productive OMS in this region during the Late Mesozoic was attributed to the influence of lower mantle under subduction asthenospheric fluid-energy columns, which intensified magma and ore-forming processes in the over subduction asthenosphere, lithosphere, and Earth's crust. This impact was most effective at stagnant oceanic slab boundaries located in the transit zone of the mantle, indicating that it was determined by deep geodynamics.

According to established theories [4,20,46,47], the impact of deep geodynamics on the Earth's crust is influenced by the decompression and dehydration processes of the oceanic slab as it moves into the mantle transition zone, followed by the advection and subsequent upwelling of fluids from the heated under subduction asthenosphere into the over subduction asthenosphere. Fluid upwelling and the resulting metasomatic transformations of the lithospheric mantle led to deformation of the lithosphere, reactivation of cratonic margin parts, and the formation of magmatogens. This sequence is evident in the locations of intermediate and peripheral magma chambers: primary chambers in the lower lithosphere within the metasomatized mantle and lower crust and associated chambers in the middle and upper parts of the Earth's crust. The intensification of magmatic and ore-forming processes has led to the development of returning mantle flows near slab boundaries and the entrapment of undepleted material from the lower mantle in ascending upper mantle plumes [32]. Given the possibility of such a scenario involving the participation of lower mantle derivatives in upper mantle plumes and subsequent mantle-crustal processes, it is logical to explain the existence of large “magmatogens”, the roots of which are located several hundred kilometers below the modern surface. The emergence of the magmatogene was accompanied by a concentration of previously dispersed elements, leading to the formation of highly productive systems. This is supported by geophysical [77], isotope geochemical [74], and computational experimental data [78].

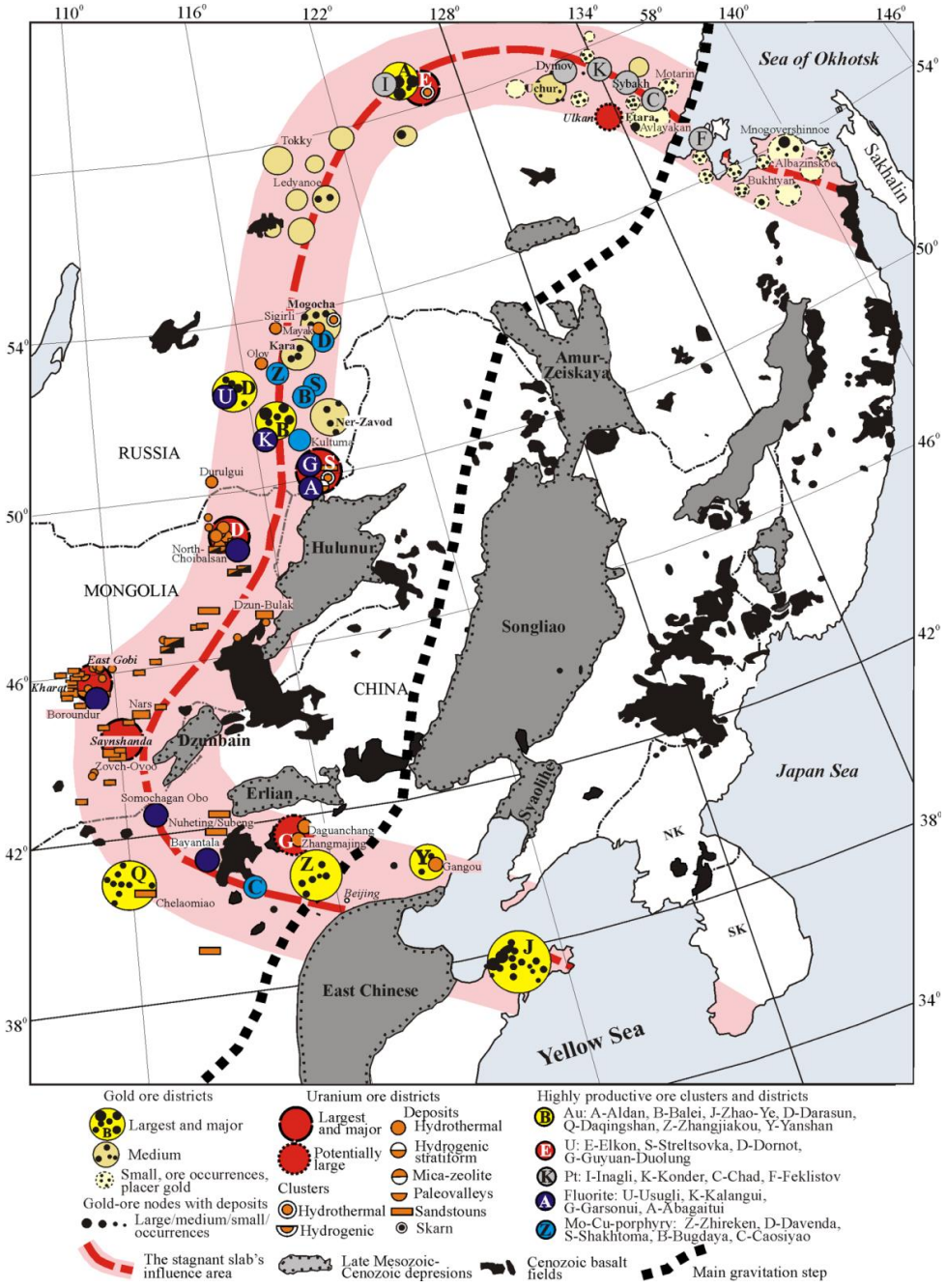

Figure 4. The location of the largest and other clusters of strategic raw materials in East Asia over a stagnant oceanic slab.

6. Conclusions

Evidence suggests the versatility of phenomena in the convergence megazone between continental and oceanic plates, accompanied by processes such as subduction, stagnation, rifting, decompression, dehydration, fluid advection, and upwelling. The emergence of return flows of lower mantle material and its mixing with upper mantle and crustal components, along with the development of a tiered system of magmatic and ore-forming chambers, explains the formation of large ore clusters and districts in East Asia (Figure 5).

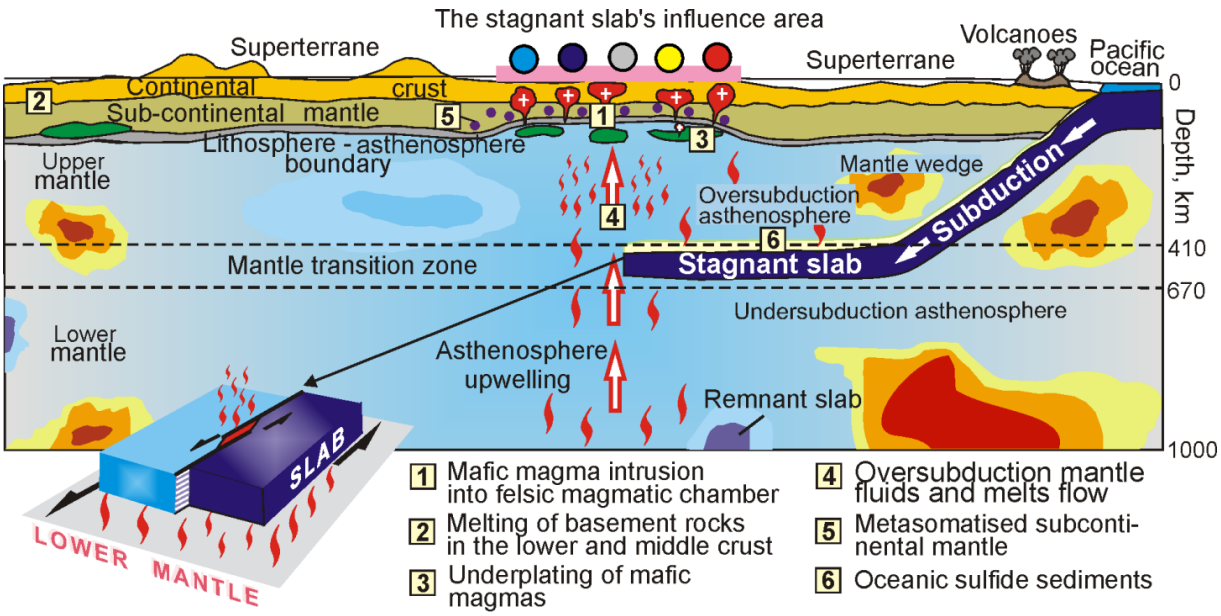

Figure 5. Geodynamic model of large ore clusters in East Asia.

The proposed model for the regular formation and placement of world-class ore districts in the cratonized crust of East Asia takes into account the influence of matter and energy from two asthenospheres and the lower mantle on the intensification of ore-forming processes. This model is supported by studies [5,6,30,79] on the localization of many other ore districts over a stagnant oceanic slab in Russia, Mongolia, and China.

Use of AI tools declaration

The author declare she have not used Artificial Intelligence (AI) tools in the creation of this article.

Acknowledgments

The article was written in memory of geologist Professor Vadim G. Khomich. The author expresses sincere gratitude for many years of productive collaboration, in particular, the scientific idea behind this research.

Conflict of interest

The author is not aware of any conflict of interest.

References

1. Khomich VG, Boriskina NG (2013) The deep geodynamics of Southeast Russia and the setting of platinum-bearing basite-hyperbasite massifs. *J Volcanolog Seismol* 7: 328–337. http://dx.doi.org/10.1134/S0742046313040040

2. Khomich VG, Boriskina NG (2014) Deep geodynamics and uranium giants of Southeastern Russia. *Dokl Earth Sci* 458: 1226–1229. http://dx.doi.org/10.1134/S1028334X14100249
3. Khomich VG, Boriskina NG, Santosh M (2018) Super large mineral deposits and deep mantle dynamics: The scenario from Southeast Trans-Baikal region, Russia. *Geol J* 53: 412–423. https://doi.org/10.1002/gj.2908
4. Khomich VG, Boriskina NG, Santosh M (2014) A geodynamic perspective of world-class gold deposits in East Asia. *Gondwana Res* 26: 816–833. https://doi.org/10.1016/j.gr.2014.05.007
5. Khomich VG, Boriskina NG, Santosh M (2015) Geodynamics of Late Mesozoic PGE, Au, and U mineralization in the Aldan shield, North Asian Craton. *Ore Geol Rev* 68: 30–42. http://dx.doi.org/10.1016/j.oregeorev.2015.01.007
6. Khomich VG, Boriskina NG (2019) Paleovolcanic necks and extrusions: Indicators of large uranium orebelts in the territories joining Russia, Mongolia, and China. *J Volcanol Geotherm Res* 383: 88–102. https://doi.org/10.1016/j.jvolgeores.2018.05.004
7. Seminskiy ZV (2021) Clusters of mineral deposits of the Southern East Siberia and prospects for their development: an overview of the problem. *Geodyn Tectonophysics* 12: 754–768.
8. Zonenshain LP, Kuzmin MI, Natapov LM (1990) *Tectonics of lithosphere plates of the USSR territory: in 2 books*, Moscow: Nedra. Available from: https://www.geokniga.org/books/6515
9. Parfenov LM, Berzin NA, Khanchuk AI, et al. (2003) Model of formation of orogenic belts of Central and North-East Asia. *Tikhookeanskaya Geologiya* 22: 7–41.
10. Shatkov GA, Volsky AS (2004) Tectonics, deep structure, and minerageny of the Amur river region and neighboring areas. St. Petersburg: VSEGEI.
11. Gordienko IV (2014) Metallogeny of various geodynamic settings of the Mongolia-Transbaikalia region. *Geol Miner Resour Sib* S3–1: 7–13.
12. Yarmolyuk VV, Kudryashov EA, Kozlovsky AM, et al. (2011) Late Cenozoic volcanic province in Central and East Asia. *Petrology* 19: 327–347. http://dx.doi.org/10.1134/S0869591111040072
13. Didenko AI, Malyshev YuF, Saksin BG (2010) *Deep structure and metallogeny of East Asia*, Vladivostok: Dalnauka. Available from: https://search.rsl.ru/ru/record/01004906622?ysclid=m2mxy27n73631732383.
14. Didenko AN, Nosyrev MY, Gil'manova GZ (2022) A gravity-derived Moho model for the Sikhote Alin orogenic belt. *Pure Appl Geophys* 179: 3967–3988. https://doi.org/10.1007/s00024-021-02842-8
15. Grachev AF (1996) The main problems of the latest tectonics and geodynamics of Northern Eurasia. *Izv Phys Solid Earth* 12: 5–36.
16. Larin AM (2014) Ulkan-Dzhugdzhur ore-bearing anorthosite-rapakivi granite-peralkaline granite association, Siberian Craton: Age, tectonic setting, sources, and metallogeny. *Geol Ore Deposits* 56: 257–280. https://doi.org/10.1134/S1075701514040047
17. Larin AM, Kotov AB, Salnikova EB, et al. (2023) Age and tectonic setting of the kopri-type granitoids at the Junction Zone of the Dzhugdzhur-Stanovoi and Western Stanovoi superterranes of the Central Asian fold belt. *Dokl Earth Sc* 509: 111–117. https://doi.org/10.1134/S1028334X22601821
18. Sorokin AA, Sorokin AP, Ponomorchuk VA, et al. (2009) Late Mesozoic volcanism of the eastern part of the Argun superterrane (Far East): Geochemistry and $^{40}Ar/^{39}Ar$ geochronology. *Stratigr Geol Correl* 17: 645–658. https://doi.org/10.1134/S0869593809060069

19. Li XC, Fan HR, Santosh M, et al. (2012) An evolving magma chamber within extending lithosphere: An integrated geochemical, isotopic and zircon U–Pb geochronological study of the Gushan granite, eastern North China Craton. *J Asian Earth Sci* 50: 27–43. https://doi.org/10.1016/j.jseaes.2012.01.016
20. Hegen Ouyang, Jingwen Mao, Zhenhua Zhou, et al. (2015) Late Mesozoic metallogeny and intracontinental magmatism, southern Great Xing'an Range, northeastern China. *Gondwana Res* 27: 1153–1172. http://dx.doi.org/10.1016/j.gr.2014.08.010
21. Zhou JB, Wilde SA, (2013) The crustal accretion history and tectonic evolution of the NE China segment of the Central Asian Orogenic Belt. *Gondwana Res* 23: 1365–1377. http://dx.doi.org/10.1016/j.gr.2012.05.012
22. Rui Zhao, Qingfei Wang, Xuefei Liu, et al. (2016) Architecture of the Sulu crustal suture between the North China Craton and Yangtze Craton: Constraints from Mesozoic granitoids. *Lithos* 266–267: 348–361. http://dx.doi.org/10.1016/j.lithos.2016.10.018
23. Larin AM, Kotov AB, Salnikova EB, et al. (2021) Age and tectonic setting of granitoids of the Uda Complex of the Dzhugdzhur block of the Stanovoy suture: new data on the formation of giant magmatic belts in Eastern Asia. *Dokl Earth Sci* 498: 362–366 https://doi.org/10.1134/S1028334X21050081
24. Fan WM, Guo F, Wang YJ, et al. (2003) Late Mesozoic calc-alkaline volcanism of post-orogenic extension in the northern Da Hinggan Mountains, northeastern China. *J Volcanol Geotherm Res* 121: 115–135. https://doi.org/10.1016/S0377-0273(02)00415-8
25. Fan HR, Hu FF, Yang JH, et al. (2007) Fluid evolution and large-scale gold metallogeny during Mesozoic tectonic transition in the Jiaodong Peninsula, eastern China. *Geol Soc London Spec Publ* 280: 303–316. https://doi.org/10.1144/SP280.16
26. Gordienko IV (2001) Geodynamic evolution of the Central-Asian and Mongol-Okhotsk fold belts and formation of the endogenic deposits. *Geosci J* 5: 233–241. https://doi.org/10.1007/BF02910306
27. Sun JG, Han SJ, Zhang Y, et al. (2013) Diagenesis and metallogenetic mechanisms of the Tuanjiegou gold deposit from the Lesser Xing'an Range, NE China: Zircon U-Pb geochronology and Lu-Hf isotopic constraints. *J Asian Earth Sci* 62: 373–388. https://doi.org/10.1016/j.jseaes.2012.10.021
28. Ren YS, Chen C, Zou XT, et al. (2016) The age, geological setting, and types of gold deposits in the Yanbian and adjacent areas, NE China. *Ore Geol Rev* 73: 284–297. https://doi.org/10.1016/j.oregeorev.2015.03.013
29. Chen YJ, Zhang C, Wang P, et al. (2017) The Mo deposits of Northeast China: A powerful indicator of tectonic settings and associated evolutionary trends. *Ore Geol Rev* 81: 602–640. http://dx.doi.org/10.1016/j.oregeorev.2016.04.017
30. Li Q, Santosh M, Li SR, et al. (2015) Petrology, geochemistry and zircon U–Pb and Lu–Hf isotopes of the Cretaceous dykes in the central North China Craton: Implications for magma genesis and gold metallogeny. *Ore Geol Rev* 67: 57–77. https://doi.org/10.1016/j.oregeorev.2014.11.015
31. Andreeva OV, Petrov VA, Poluektov VV (2020) Mesozoic acid magmatites of Southeastern Transbaikalia: petrogeochemistry and relationship with metasomatism and ore formation. *Geol Ore Deposits* 62: 69–96. https://doi.org/10.1134/S1075701520010018

32. Zhao D, Pirajno F, Dobretsov NL, et al. (2010) Mantle structure and dynamics under East Russia and adjacent regions. *Russ Geol Geophys* 51: 925–938. https://doi.org/10.1016/j.rgg.2010.08.003
33. Deng J, Wang Q (2016) Gold mineralization in China: Metallogenic provinces, deposit types and tectonic framework. *Gondwana Res* 36: 219–274. https://doi.org/10.1016/j.gr.2015.10.003
34. Zonenshain LP, Savostin LA (1981) Geodynamics of the Baikal Rift System and Plate Tectonics of Asia. *Tectonophysics* 76: 1–45. https://doi.org/10.1016/0040-1951(81)90251-1
35. Kepezhinskas PK, Kepezhinskas NP, Berdnikov NV, et al. (2020) Native metals and intermetallic compounds in subduction-related ultramafic rocks from the Stanovoy mobile belt (Russian Far East): implications for redox heterogeneity in subduction zones. *Ore Geol Rev* 127: 103800. https://doi.org/10.1016/j.oregeorev.2020.103800
36. Kepezhinskas P, Berdnikov N, Kepezhinskas N, et al. (2022) Adakites, high-Nb basalts and copper-gold depositions in magmatic arcs and collictional orogens: an overview. *Geosciences* 12: 29. https://doi.org/10.3390/geosciences12010029
37. Malyshev YF, Podgornyi VY, Shevchenko BF, et al. (2007) Deep structure of the Amur lithospheric plate border zone. *Russ J Pac Geol* 1: 107–119. https://doi.org/10.1134/S1819714007020017
38. Maruyama S, Santosh M, Zhao D (2007) Superplume, supercontinent, and post-perovskite: Mantle dynamics and antiplate tectonics on the Core-Mantle Boundary. *Gondwana Res* 11: 7–37. http://dx.doi.org/10.1016/j.gr.2006.06.003
39. Li C, van der Hilst RD (2010) Structure of the upper mantle and transition zone beneath Southeast Asia from traveltime tomography. *J Geophys Res Solid Earth* 115: B07308. https://doi.org/10.1029/2009JB006882
40. Li J, Wang X, Wang X, et al. (2013) P and SH velocity structure in the upper mantle beneath Northeast China: Evidence for a stagnant slab in hydrous mantle transition zone. *Earth Planet Sci Lett* 367: 71–81. https://doi.org/10.1016/j.epsl.2013.02.026
41. Zhao D, Tian Y (2013) Changbai intraplate volcanism and deep earthquakes in East Asia: a possible link? *Geophys J Int* 195: 706–724.
42. Jiang G, Zhang G, Zhao D, et al. (2015) Mantle dynamics and cretaceous magmatism in east-central China: Insight from teleseismic tomograms. *Tectonophysics* 664: 256–268. http://dx.doi.org/10.1016/j.tecto.2015.09.019
43. Khomich VG, Boriskina NG, Kasatkin SA (2019) Geology, magmatism, metallogeny, and geodynamics of the South Kuril Islands. *Ore Geol Rev* 105: 151–162. https://doi.org/10.1016/j.oregeorev.2018.12.015
44. Khomich VG, Boriskina NG, Santosh M (2016) Geodynamic framework of large unique uranium orebelts in Southeast Russia and East Mongolia. *J Asian Earth Sci* 119: 145–166. http://dx.doi.org/10.1016/j.jseaes.2016.01.018
45. Khutorskoi MD, Polyak BG (2017) Special features of heat flow in transform faults of the North Atlantic and Southeast Pacific. *Geotectonics* 51: 152–162. https://doi.org/10.1134/S0016852117010022
46. Goldfarb RJ, Santosh M (2014) The dilemma of the Jiaodong gold deposits: are they unique? *Geosci Front* 5: 139–153. http://dx.doi.org/10.1016/j.gsf.2013.11.001

47. Mao XC, Ren J, Liu ZK, et al. (2019) Three-dimensional prospectivity modeling of the Jiaojia-type gold deposit, Jiaodong Peninsula, Eastern China: A case study of the Dayingezhuang deposit. *J Geochem Explor* 203: 27–44. https://doi.org/10.1016/j.gexplo.2019.04.002
48. Chen Y, Guo G, Li X (1998) Metallogenic geodynamic background of Mesozoic gold deposits in granite-greenstone terrains of North China Craton. *Sci China Ser D-Earth Sci* 41: 113–120. https://doi.org/10.1007/BF02932429
49. Zorin YA, Turutanov EK, Kozhevnikov VM, et al. (2006) On the nature of Cenozoic upper mantle plumes in Eastern Siberia (Russia) and Central Mongolia. *Russ Geol Geophys* 47: 1056–1070.
50. Khomich VG, Boriskina NG (2009) Relationship between the gold bearing areas and gradient sones of the gravity field of southeastern regions of Russia. *Dokl Earth Sc* 428: 1100–1104. http://dx.doi.org/10.1134/S1028334X09070137
51. Laverov NP, Velichkin VI, Vlasov BP, et al. (2012) Uranium and molybdenum-uranium deposits in the areas of continental intracrustal magmatism: geology, geodynamic and physico-chemical conditions of formation. Moscow: IFSN RAN IGEM RAN.
52. Berzina AP, Berzina AN, Gimon VO, et al. (2015) The Zhireken porphyry Mo ore-magmatic system (Eastern Transbaikalia): U-Pb age, sources, and geodynamic setting. *Russ Geol Geophys* 56: 446–465. https://doi.org/10.1016/j.rgg.2015.02.006
53. Mashkovtsev GA, Korotkov VV, Rudnev VV (2020) Ore-bearing of the Mesozoic tectonic-magmatic activation area of the Eastern Siberia and the Far East. *Prospect Prot Miner Resour* 11: 5–7.
54. Vetluzhskikh VG, Kazansky VI, Kochetkov AY, et al. (2002) Central Aldan gold deposits. *Geol Ore Deposits* 44: 405–434. Available from: https://www.pleiades.online/cgi-perl/search.pl?type=abstract&name=geolore&number=6&year=2&page=405.
55. Shatov VV, Molchanov AV, Shatova NV, et al. (2012) Petrography, geochemistry and isotopic (U-Pb and Rb-Sr) dating of alkaline magmatic rocks of the Ryabinovy massif (South Yakutia). *Reg Geol Metallog* 51: 62–78.
56. Chernyshev IV, Prokof'ev VY, Bortnikov NS, et al. (2014) Age of granodiorite porphyry and beresite from the Darasun gold field, Eastern Transbaikal region, Russia. *Geol Ore Deposits* 56: 1–14. https://doi.org/10.1134/S1075701514010036
57. Andreeva OV, Golovin VA, Kozlova PS, et al. (1996) Evolution of mesozoic magmatism and ore-forming metasomatic processes in the Southeastern Transbaikal region (Russia). *Geol Ore Deposits* 38: 101–113.
58. Stupak FM, Kudryashova EA, Lebedev VA, et al. (2018) The structure, composition, and conditions of generation for the early cretaceous Mongolia—East-Transbaikalia volcanic belt: the Durulgui–Torei area (Southern Transbaikalia, Russia). *J Volcanolog Seismol* 12: 34–46. https://doi.org/10.1134/S0742046318010074
59. Ponomarchuk AV, Prokopyev IR, Svetlitskaya TV, et al. (2019) $^{40}Ar/^{39}Ar$ geochronology of alkaline rocks of the Inagli massif (Aldan Shield, Southern Yakutia). *Russ Geol Geophys* 60: 33–44. https://doi.org/10.15372/RGG2019003

60. Gaskov IV, Borisenko AS, Borisenko ID, et al. (2023) Chronology of alkaline magmatism and gold mineralization in the Central Aldan ore district (Southern Yakutia). *Russ Geol Geophys* 64: 175–191. https://doi.org/10.2113/RGG20214427
61. Shukolyukov YA, Yakubovich OV, Mochalov AG, et al. (2012) New geochronometer for the direct isotopic dating of native platinum minerals (^{190}Pt-^{4}He method). *Petrology* 20: 491–505. http://dx.doi.org/10.1134/S0869591112060033
62. Ronkin YL, Efimov AA, Lepikhina GA, et al. (2013) U-Pb dating of the baddeleytte-zircon system from Pt-bearing dunite of the Konder massif, Aldan Shield: New data. *Dokl Earth Sc* 450: 607–612. https://doi.org/10.1134/S1028334X13060135
63. Mochalov AG, Yakubovich OV, Bortnikov NS (2016) ^{190}Pt–^{4}He age of PGE ores in the alkaline–ultramafic Konder massif (Khabarovsk district, Russia). *Dokl Earth Sc* 469: 846–850. https://doi.org/10.1134/S1028334X16080134
64. Mochalov AG, Yakubovich OV, Bortnikov NS (2022) ^{190}Pt–^{4}He dating of placer-forming minerals of platinum from the Chad alkaline-ultramafic massif: new evidence of the polycyclic nature of ore formation. *Dokl Earth Sc* 504: 240–247. https://doi.org/10.1134/S1028334X22050105
65. Kazansky VI (2004) The unique Central Aldan gold-uranium ore district (Russia). *Geol Ore Deposits* 46: 167–181.
66. Mashkovtsev GA, Konstantinov AK, Miguta AK, et al. (2010) Uranium of Russian entrails, Moscow: VIMS. Available from: https://elib.biblioatom.ru/text/uran-rossiyskih-nedr_2010/p0/.
67. Afanasyev GV, Mironov YB, Pinsky EM (2018) Role of combined paleohydrogeological systems in forming uranium mineralization in volcano-tectonic depressions of the Central Asian mobile belt. *Reg Geol Metallog* 3: 77–87.
68. Rui GZ (2010) Discussion on the geological characteristics and origin of the 460 large uranium-molybdenum deposit. *World Nucl Geol* 27: 149–154.
69. Wu JH, Ding H, Niu ZL, et al. (2015) SHRIMP zircon U-Pb dating of country rock in Zhangmajing U-Mo deposit in Guyuan, Hebei Province, and its geological significance. *Mineral Deposit* 4: 757–768.
70. Wang JQ, Liu GJ, Dong S, et al. (2023) The "trinity" prospecting prediction geological model of the Zhangmajing uranium molybdenum deposit in Guyuan County, Hebei Province. *Geol Bull China* 42: 931–940. http://dx.doi.org/10.12097/j.issn.1671-2552.2023.06.006
71. Rybalov BL (2000) Evolutionary rows of Late Mesozoic ore deposits of the Eastern Transbaikal region (Russia). *Geol Ore Deposits* 42: 340–350.
72. Berzina AP, Berzina AN, Gimon VO (2014) Geochemical and Sr–Pb–Nd isotopic characteristics of the Shakhtama porphyry Mo-Cu system (Eastern Transbaikalia, Russia). *J Asian Earth Sci* 79: 655–665. http://dx.doi.org/10.1016/j.jseaes.2013.07.028
73. Berzina AP, Berzina AN, Gimon VO (2016) Paleozoic-Mesozoic porphyry Cu (Mo) and Mo (Cu) deposits within the southern margin of the Siberian Craton: geochemistry, geochronology, and petrogenesis (a Review). *Minerals* 6: 125. http://dx.doi.org/10.3390/min6040125
74. Pushkarev YD, Kostoyanov AI, Orlova MP, et al. (2002) Features of Rb-Sr, Sm-Nd, Pb-Pb, Re-Os and K-Ar isotope systems in the Konder massif: mantle substrate enriched in platinum group metals. *Reg Geol Metallog* 16: 80–91.

75. Simonov VA, Prikhodko VS, Kovyazin SV (2011) Genesis of platiniferous massifs in the Southeastern Siberian platform. *Petrology* 19: 549–567. http://dx.doi.org/10.1134/S0869591111050043
76. Shatkov GA, Antonov AV, Butakov PM, et al. (2014) Uranyl molybdates in fluorites and uranium-carbonate ores from the Streltsovskoe ore field of the Argun deposit. *Dokl Earth Sc* 456: 764–768. https://doi.org/10.1134/S1028334X14060373
77. Konstantinov MM, Politov VK, Novikov VP, et al. (2002) Geological structure of gold districts of volcano-plutonic belts in Eastern Russia. *Geol Ore Deposits* 44: 252–266.
78. Dobretsov NL, Koulakov I, Kukarina EV, et al. (2015) An integrate model of subduction: contributions from geology, experimental petrology, and seismic tomography. *Russ Geol Geophys* 56: 13–38. https://doi.org/10.1016/j.rgg.2015.01.002
79. Pechenkin IG (2016) Relationship between uranium metallogeny and geodynamic processes in the marginal parts of Eurasia. *Ores Metals* 2: 5–17.

AIMS Press